

Multiscale velocity correlation in turbulence : experiments, numerical simulations, synthetic signals

Citation for published version (APA):

Benzi, R., Biferale, L., Ruiz-Chavarria, G., Ciliberto, S., & Toschi, F. (1999). Multiscale velocity correlation in turbulence : experiments, numerical simulations, synthetic signals. *Physics of Fluids*, 11(8), 2215-2224. <https://doi.org/10.1063/1.870083>

DOI:

[10.1063/1.870083](https://doi.org/10.1063/1.870083)

Document status and date:

Published: 01/01/1999

Document Version:

Publisher's PDF, also known as Version of Record (includes final page, issue and volume numbers)

Please check the document version of this publication:

- A submitted manuscript is the version of the article upon submission and before peer-review. There can be important differences between the submitted version and the official published version of record. People interested in the research are advised to contact the author for the final version of the publication, or visit the DOI to the publisher's website.
- The final author version and the galley proof are versions of the publication after peer review.
- The final published version features the final layout of the paper including the volume, issue and page numbers.

[Link to publication](#)

General rights

Copyright and moral rights for the publications made accessible in the public portal are retained by the authors and/or other copyright owners and it is a condition of accessing publications that users recognise and abide by the legal requirements associated with these rights.

- Users may download and print one copy of any publication from the public portal for the purpose of private study or research.
- You may not further distribute the material or use it for any profit-making activity or commercial gain
- You may freely distribute the URL identifying the publication in the public portal.

If the publication is distributed under the terms of Article 25fa of the Dutch Copyright Act, indicated by the "Taverne" license above, please follow below link for the End User Agreement:

www.tue.nl/taverne

Take down policy

If you believe that this document breaches copyright please contact us at:

openaccess@tue.nl

providing details and we will investigate your claim.

Multiscale velocity correlation in turbulence: Experiments, numerical simulations, synthetic signals

R. Benzi

AIPA, Via Po 14, 00100 Roma, Italy

L. Biferale

*Dipartimento di Fisica, Università di Tor Vergata, Via della Ricerca Scientifica 1, I-00133 Roma, Italy
and INFM-Unità di Tor Vergata, Roma, Italy*

G. Ruiz-Chavarría

Departamento de Física, Facultad de Ciencias, UNAM 04510 Mexico D.F., Mexico

S. Ciliberto

*Laboratoire de Physique, URA 1325, Ecole Normale Supérieure de Lyon, 46 Allée d'Italie,
69364 Lyon, France*

F. Toschi

*INFM-Unità di Tor Vergata, Roma, Italy and Dipartimento di Fisica, Università di Pisa,
Piazza Torricelli 2, I-56126 Pisa, Italy*

(Received 23 September 1998; accepted 3 May 1999)

Multiscale correlation functions in high Reynolds number experimental turbulence, numerical simulations, and synthetic signals are investigated. Fusion Rules predictions as they arise from multiplicative, almost uncorrelated, random processes for the energy cascade are tested. Leading and subleading contribution, in the inertial range, can be explained as arising from a multiplicative random process for the energy transfer mechanisms. Two different predictions for correlations involving dissipative observable are also briefly discussed. © 1999 American Institute of Physics. [S1070-6631(99)04208-7]

I. INTRODUCTION

Understanding the statistical properties of intermittency is one of the most challenging open problem of three-dimensional fully developed turbulence.

Intermittency in the inertial range is usually analyzed by means of the statistical properties of velocity differences, $\delta_r v(x) = v(x+r) - v(x)$. In the following, being mainly interested in one-dimensional cuts of experimental, synthetic, and numerical signals, we will disregard all vectorial dependencies in the velocity fields.

In the last 20 years,¹ overwhelming experimental and theoretical works focused on structure functions, $S_p(r) = \langle (\delta_r v(x))^p \rangle$. A wide agreement exists on the fact that structure functions show a scaling behavior in the limit of very high Reynolds numbers, i.e., in the presence of a large separation between integral and dissipative scales, $L/r_d \rightarrow \infty$,

$$S_p(r) \sim \left(\frac{r}{L}\right)^{\zeta(p)}. \quad (1)$$

The velocity fluctuations are anomalous in the sense that $\zeta(p)$ exponents do not follow the celebrated dimensional prediction made by Kolmogorov, $\zeta(p) = p/3$. In fact, $\zeta(p)$ are observed to be a nonlinear function of p , which is the most important signature of the intermittent transfer of fluctuations from large to small scales.

In order to better characterize the transfer mechanism, it is natural to look also at correlations among velocity fluctuations at different scales and at different times. The prototype of such a class of correlations is

$$C_{p,q}(r, R; \tau) = \langle (\delta_r v(x, t))^p (\delta_R v(x, t + \tau))^q \rangle, \quad (2)$$

where, hereafter we will always assume the obvious notation, $r < R$.

Unfortunately, the nontrivial time dependency of correlations such as (2) is completely hidden, in a Eulerian reference-frame, by the sweeping of small scales by large scales. The “positive” side of sweeping is connected to the Taylor hypothesis, i.e., to the possibility of identifying single point measurements at a time delay τ with single time measurements at separation scale $r \sim \tau \bar{V}$, where \bar{V} is the large scale sweeping velocity. The “negative” side of sweeping is connected to the fact that the inertial time scales are always subdominant with respect to the sweeping time. This implies that in order to measure the temporal properties of the inertial range energy-transfer it is necessary to abandon the usual Eulerian reference-frame and to move in a Lagrangian or quasi-Lagrangian reference-frame where sweeping effects are absent.^{2,3,5,7,9} Of course, from the experimental point of view, it is much harder to measure the velocity field in a Lagrangian frame than in the usual laboratory reference-frame. To our knowledge, the only results about multi-time velocity correlations are purely theoretical^{5,9} or numerical.^{4,5} For this reason, in the following, we will limit to an experi-

mental and theoretical analysis of simultaneous -single time-multiscale correlation functions only. Recently, some theoretical work⁶⁻⁹ and an exploratory experimental investigation¹⁰ have been devoted to the behavior of single-time multiscale velocity correlations (MSVC),

$$F_{p,q}(r,R) \equiv \langle (v(x+r) - v(x))^p (v(x+R) - v(x))^q \rangle \\ \equiv \langle (\delta_r v(x))^p (\delta_R v(x))^q \rangle, \quad (3)$$

with $r_d < r < R < L$. When the smallest among the two scales r goes beyond the dissipative scales, r_d , new properties of the correlation functions (3) may arise due to the nontrivial physics of the dissipative cutoff.^{1,11} From now on, we will mostly concentrate on correlation functions with both r and R in the inertial range, only in the last section we will address the important point concerned with the crossover of the dissipative scale. Moreover, in order to simplify our discussion, we will confine our analysis to the case of longitudinal velocity differences.

The main purpose of this paper is to review and to extend a recent experimental and theoretical analysis of multiscale correlations (3).¹⁶ In particular, we present a systematic analysis of multiscale correlation functions in different experimental setup, we also perform a critical comparison with the same observable measured in synthetic turbulent signals defined in terms of purely multiplicative random processes.

The comparison with the synthetic signals will allow us to conclude that multiscale correlation functions are in *quantitative* agreement, with the prediction one obtains by using a pure uncorrelated multiplicative process for the energy cascade, as long as both separations r, R are in the inertial range. As for the case when one of the two separations is already in the dissipative range we will critically review the two most important different predictions one can obtain imposing the dissipative cut-off using either multifractals¹⁵ or the GESS phenomenology.¹¹ Unfortunately, the actual state-of-the-art experimental dissipative-scales data does not allow to clearly distinguish among the two predictions.^{12,13}

The paper is organized as follows. In Sec. II we briefly review the *ansatz* that one simply obtains for MSVC (3) by using a multiplicative random process for the inertial-range energy cascade. In Sec. III we discuss subleading corrections induced by geometrical constraints which necessarily affects any MSVC for finite separation of scales. These geometrical constraints introduce subleading power laws behavior which may strongly interfere with the leading multiplicative predictions for finite separation of scales $r/R \sim O(1)$. In Sec. III we also present our experimental data-analysis and the comparison with the synthetic multifractal field. In Sec. IV we briefly address the problem of dissipative correlation functions. Conclusions follow in Sec. V.

II. CASCADE PROCESSES

Stochastic cascade processes are simple and well known useful tools to describe the leading phenomenology of the intermittent energy transfer in the inertial range. Both anomalous scaling exponents and viscous effects^{1,11} can be

reproduced by choosing a suitable random process for the multiplier, $W(r, R)$, which connects velocity fluctuations at two different scales, $R > r$.

The main idea turns around the hypothesis that small scale statistics is fully determined by a cascade process conditioned to some large scale configuration,

$$\delta_r v(x) = W(r, R) \cdot \delta_R v(x), \quad (4)$$

where, requiring homogeneity along the cascade process, the random function W should depend only on the ratio r/R and it is not-positive defined. In the hypothesis of negligible correlations among multipliers we obtain

$$F_{p,q}(r,R) = C_{p,q} \left\langle \left[W\left(\frac{r}{R}\right) \right]^p \right\rangle \left\langle \left[W\left(\frac{R}{L}\right) \right]^{p+q} \right\rangle \\ \sim \frac{S_p(r)}{S_p(R)} S_{p+q}(R). \quad (5)$$

This expression was for the first time proposed in Ref. 6 and later examined in more details in Ref. 7, where it was named ‘‘fusion rules.’’ In the same article the authors proved that the fusion rule prediction gives the leading behavior of (3) when $r/R \rightarrow 0$ as long as some hypothesis of scaling invariance and of universality of scaling exponents in Navier–Stokes equations hold. The name fusion-rules refers, probably, to the fact that thanks to the—supposed—uncorrelated nature of the cascade process every multiscale correlation can be written in terms of single scale correlations, i.e., structure functions.

Let us notice that, beside any rigorous claim, expression (5) is also the zeroth order prediction starting from any multiplicative uncorrelated random cascade satisfying $S_p(r) = \langle [W(r/R)]^p \rangle S_p(R)$. Let us also stress that the fusion rules prediction as stated in (5) does not necessarily require any scaling property of the underlying structure functions, a fact which suggests that the validity of the statement should be almost Reynolds independent.

In this paper we want to address three main questions; (i) whether the prediction (5) gives the correct leading behavior in the limit of large scales separation: $r/R \sim 0$; (ii) if this is the case, what one can say about subleading behavior for separation $r/R \sim O(1)$; (iii) what happens to those observable for which the ‘‘multiplicative prediction;’’ (5) is incorrect because of symmetry reasons.

The last item comes from the observation that for correlation like

$$F_{1,q}(r,R) = \langle (\delta_r v)(\delta_R v)^q \rangle, \quad (6)$$

the multiplicative prediction gives

$$F_{1,q}(r,R) = \frac{S_1(r)}{S_1(R)} \cdot S_{1+q}(R).$$

Such a prediction is wrong because, if homogeneity can be assumed, $S_1(r) \equiv 0$ for all scales r . In this case prediction (5) does not represent the leading contribution.

In the following we propose a systematic investigation of (3) in high Reynolds number experiments,^{17,18} numerical simulation,¹⁹ and synthetic signals.¹⁴ The main purpose consists in probing whether multiscale correlation functions may

show new dynamical properties (if any) which are not taken into account by the standard simple multiplicative models for the energy transfer.

III. DATA ANALYSIS

In this section we present our main contributions by discussing the three items listed in the previous section and by presenting a detailed data-analysis in experiments at different Reynolds numbers, in numerical simulations and in synthetic signals.

Experimental data sets come mainly from two different laboratories. We have analyzed data obtained in a wind tunnel (Modane) with $Re_\lambda=2000$, the integral scale was $L \sim 20$ m and the dissipative scale was $r_d=0.31$ mm. The second data set comes from a recirculating wind tunnel (ENS de Lyon) with a working section 3 m long and 50×50 cm² cross section. Re_λ involved in experiments were 400 (wake behind a cilinder) and 800 (jet turbulence). Integral scales were 0.1 m and 0.125 m, respectively, whereas the dissipative scales were 0.15 mm and 0.1 mm.

Synthetic signals are built in terms of a Wavelet decomposition with coefficients defined by a pure uncorrelated random multiplicative process.¹⁴ In the following, the comparison between the synthetic field and the experimental data will play a central role in our discussion. Therefore, in the Appendix, we briefly recall how a multiaffine field may be synthesized—and analyzed—in terms of a wavelet representation.

In the Appendix we prove that such a signal shows the fusion rules prediction (5) and therefore it will turn out to be an useful tool for testing how much deviations from (5), observed in experiments or numerical simulations, are due to important dynamical effects or only to unavoidable geometrical corrections. Let us proceed with a simple but basic observation.

Notice that for any one-dimensional string of number (such as the typical outcome of laboratory experiments in turbulence) the multiscale correlations (3) feel unavoidable strong geometrical constraints. In particular, for any MSVC, with two velocities at the same spatial point $v(x)$ and the two other velocities in a collinear geometry at spatial locations $v(x+r)$ and $v(x+R)$, like those analyzed in the following, we will always write down what we like to call the “ward-identities” (WI),

$$S_p(R-r) \equiv \langle [(v(x+R) - v(x)) - (v(x+r) - v(x))]^p \rangle \quad (7)$$

$$= \sum_{k=0,p} b(k,p) (-1)^k F_{k,p-k}(r,R), \quad (8)$$

where $b(k,p) = p!/[k!(p-k)!]$. For example, for $p=2$ we have

$$2F_{1,1}(r,R) \equiv S_2(r) + S_2(R) - S_2(R-r) \sim \left[\left(\frac{r}{R} \right)^{\zeta(2)} + O\left(\frac{r}{R} \right) \right] \cdot S_2(R), \quad (9)$$

where the latter expression has been obtained by expanding $S_2(R-r)$ in the limit $r/R \rightarrow 0$.

The “ward-identities” will turn out to be useful for understanding subleading predictions to the multiplicative cascade process. One may argue that in a geometrical setup different from the one specified in (3) the same kind of constraint will appear with eventually different weights among different terms.

The most important result one must extract from (8) is that the multiscale correlation functions, as stated in (3), may not be a perfect scaling functions even in the limit of very high Reynolds number. Indeed, the WI tell us that MSVC with different order of velocity moments must be connected unavoidably one with the other, which would be in contrast with the assumption that each MSVC should be determined by a single power law behavior.

The main result presented in this work is that all multiscale correlations functions are well reproduced in their leading term, $r/R \rightarrow 0$, by a simple uncorrelated random cascade (5) and that their subleading contribution, $r/R \sim O(1)$, are fully captured by the geometrical constrained previously discussed, namely the “ward-identities.”

The recipe for calculating multiscale correlations is the following: First, apply the multiplicative guess for the leading contribution and look for geometrical constraints in order to find out sub-leading terms. Second, in all cases where the leading multiplicative contribution vanishes because of underlying symmetries, look directly for the geometrical constraints and find out what is the leading contribution applying the multiplicative random approximation to all, nonvanishing, terms in the WI.

A. Fusion rules: Even moments

Let us check the fusion rules prediction (5) for even moments $p,q=2,4,\dots$. In order to better highlight the scaling properties we will often use in the following, $\bar{F}_{p,q}(r,R)$, the MSVC compensated with the fusion-rule prediction,

$$\bar{F}_{p,q}(r,R) = \frac{F_{p,q}(r,R) \cdot S_p(R)}{S_p(r) \cdot S_{p+q}(R)}. \quad (10)$$

In order to compare experiments with different Reynolds numbers we may use as independent variable in our plot the quantity, $x(R) \equiv (R-r)/(L-r)$, where with L we intend the integral scale of each different experiment. In this way, by fixing the small scale $r=5\eta$ and by changing $r \leq R \leq L$ for each set of data we have a variation of $0 \leq x(R) \leq 1$. In Fig. 1 we have checked the large scale dependency by plotting the compensated MSVC as a function of $x \equiv (R-r)/(L-r)$ at fixed, r , for $p=2, q=2$ and different Reynolds numbers (experimental and numerical). Expression (5) predicts the existence of a *plateau* (independent of R) at all scales $r \leq R \leq L$, where the leading multiplicative description is correct.

From Fig. 1 one can see that experiments with low Re numbers show a slightly poor *plateau*. In particular the direct numerical simulation (DNS) with $Re_\lambda \sim 40$ does not show any *plateau*. The absence of a *plateau* is connected to the overwhelming geometrical effects present at such low Reynolds numbers (see below). For this reason, in the following figures we will show only experimental data from Modane

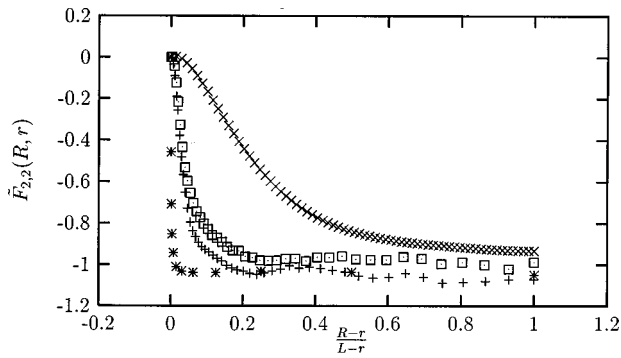


FIG. 1. Compensated MSVC $\tilde{F}_{2,2}(r, R)$ at fixed r and changing $x(R)=(R-r)/(L-r)$ for different experiments and numerical simulation: (x) direct numerical simulation ($Re_\lambda=40$), (+) jet ($Re_\lambda=800$), (*) modane ($Re_\lambda=2000$), (\square) wake ($Re_\lambda=400$). Typical statistics are 100 eddy turn over times for the DNS, and 50 eddy turn over times for the experimental signals.

wind tunnel, which have the highest Re number we can access.

In Fig. 2(a) we plot structure functions of order 2 and 4 for the highest Reynolds number data we had. As it is possible to see, a quantitative good agreement with the accepted high-Reynolds number intermittent scaling is detectable for almost two decades. On the other hand, in Fig. 2(b) we plot the multiscale correlation function $F_{2,2}(r, R)$ and $F_{2,4}(r, R)$ as a function of R at fixed r . As it is possible to see the scaling is not as clear as was for the single-scale structure function and indeed it is impossible to extract any quantitative measurements about scaling exponents even at such as high Reynolds numbers ($Re_\lambda=2000$). As already stated above, in order to better appreciate the violation to the fusion-rule scaling we plot in Fig. 2(c) the compensated correlation functions for two different set of moments. In the limit of large separation $R \rightarrow L$ at fixed r , we indeed see a tendency toward a *plateau*. On the other hand, there are clear deviations for $r/R \sim O(1)$. The same behavior is seen in Fig. 3 for the same compensated quantities fixing the large scale R and by changing the small scale r . Such deviations show a very slow decay as a function of the scale separation. The decaying is so slow that a clear *plateau* is seen only for the largest Reynolds number available. The question whether the observed finite-size corrections have an important physical origin or not is therefore of primary importance.

In order to understand the physical meaning of the observed deviations to the fusion rules (5), we compare, in Fig. 4, the experimental data against the equivalent quantities measured by using the synthetic signal.

We notice an almost perfect superposition of the two data sets, indicating that the deviations observed in real data can hardly be considered a “dynamical effect.” For dynamical effect we mean a correlation of the energy cascade which must be incorporated in the statistical properties of the multiplicative process.

Using the WI plus the multiplicative *ansatz* for the leading behavior of all correlation functions for $p=4$ we quickly read that the leading contribution to $F_{2,2}$ is $O(r^{\xi(2)}) \cdot O(R^{\xi(4)-\xi(2)})$, while subleading terms scale as $O(r^{\xi(4)})$,

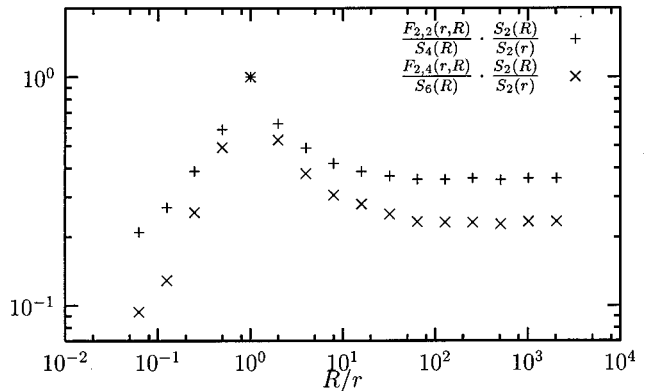
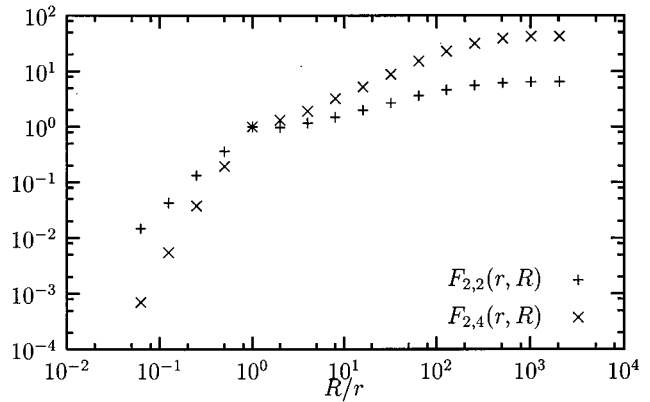
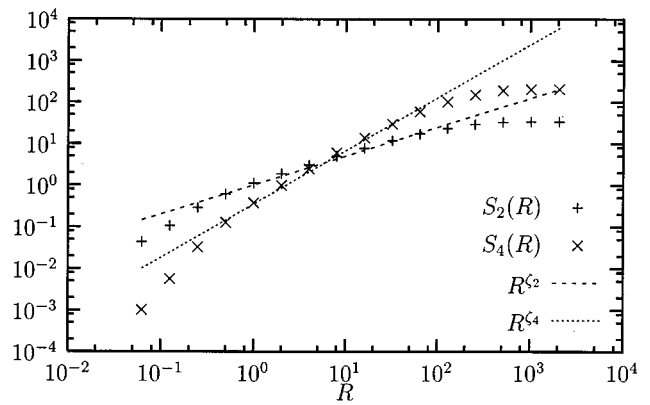


FIG. 2. (a) Log–log plot of the second order, $S_2(R)$, and fourth order, $S_4(R)$, structure functions with superimposed the straight line expected for the corresponding high-Reynolds number intermittent scalings. x -scale is in unity of 16 Kolmogorov scales, y -units are arbitrary. (b) Log–log plot of the two-scale correlation function $F_{2,2}(r, R)$ (+) and $F_{2,4}(r, R)$ (x) at fixed r and at changing R . The small scale r is fixed to be 16 Kolmogorov scales. Units are as in (a). (c) Compensated MSVC $\tilde{F}_{p,q}(r, R)$ at fixed r and changing the large scale R for $p=2, q=2$ (+) and $p=2, q=4$ (x). Units are as in (b).

and as $O(r^{\xi(3)}) \cdot O(R^{\xi(4)-\xi(3)})$. This superposition of power laws is responsible for the slowly-decaying correlations in Figs. 1–4.

In Table I we summarize the leading and subleading contributions that may be inferred from the WI for the standard MSVC with $p=2, q=2$. Similar tables can be constructed for any other even MSVC.

The result so far obtained, i.e., that both the experimental data and the synthetic signal show the same quantitative

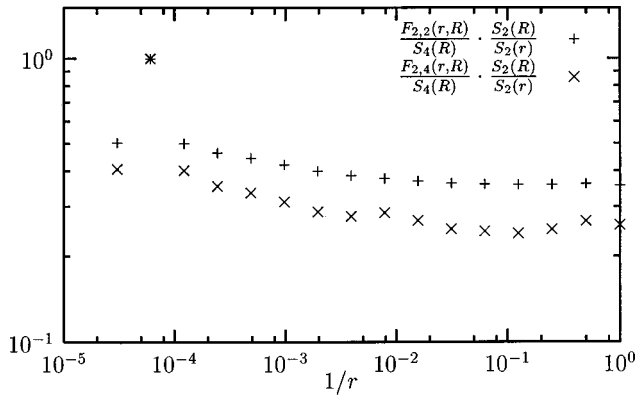


FIG. 3. Experimental compensated MSVC $F_{p,q}(r,R)/S_{p+q}(R) \cdot S_p(r)$ at fixed R and changing the small scale $1/r$ for $p=2, q=2$ (+) and $p=2, q=4$ (x).

behavior, is a strong indication that multiscale correlation functions, at least for even order of the moments, i.e., in all cases where the signal is not affected by cancellation problems, are in good agreement with the random multiplicative model for the energy transfer.

An even stronger proof of this statement comes from the analysis of multiscale correlations in terms of the coefficients obtained by a Wavelet analysis of the experimental signal (see Appendix). The Wavelet coefficient $\alpha_{j,k}$ may be seen as the representative of a velocity fluctuation at scale $r=2^{-j}$ and centered in one of the $k=1,2,\dots,2^j$ spatial point chosen equispaced in the original total length of the signal.

With this interpretation in mind, we may think at the Wavelet coefficients as the ideal observable which minimize the geometrical constraints and therefore as the ideal cases where one can test the idea that behind the multiplicative process there are only geometrical constraints. In other words, in terms of the coefficients obtained by a wavelet analysis of the experimental signal, the multiscale correlation function should show the fusion rules prediction for a range of scales much wider than for the velocity increments, i.e., geometrical constraints, which introduce subleading power-laws decaying, should be minimized. Of course the degree of elimination of geometrical constraints may depend on the

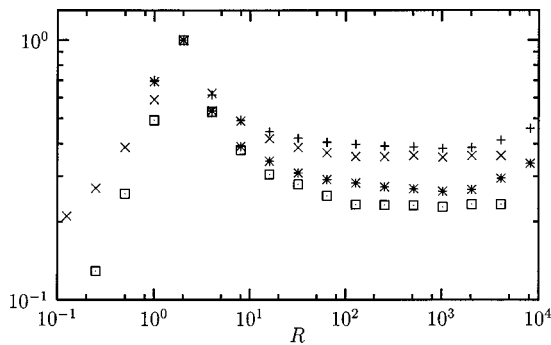


FIG. 4. Comparison between experimental and synthetic compensated MSVC, $\bar{F}_{p,q}(r,R)$ at fixed r and changing the large scale R for $p=2, q=2$: (+) synthetic and (x) experimental. For $p=2, q=4$: (*) synthetic and (□) experimental.

TABLE I. Leading (first column) and subleading (second column) contribution to the different multiscale velocity correlations entering in the WI written for $p=4$. Notice that all the leading behaviors have been obtained by using the multiplicative *ansatz* (when applicable). The subleading behaviors are consistent with the constraints imposed by the WI.

	Leading	Subleading
$S_4(R-r)$	$R^{\zeta(4)}$	$\frac{r}{R} R^{\zeta(4)}$
$F_{3,1}(r,R)$	$r^{\zeta(3)} R^{\zeta(4)-\zeta(3)}$	$\frac{r}{R} R^{\zeta(4)}$
$F_{1,3}(r,R)$		$S_4(R-r), F_{3,1}(r,R)$
$F_{2,2}(r,R)$	$r^{\zeta(2)} R^{\zeta(4)-\zeta(2)}$	$r^{\zeta(3)} R^{\zeta(4)-\zeta(3)}, \frac{r}{R} R^{\zeta(4)}$

kind of analyzing wavelets used. For instance by analyzing the synthetic signal with the same kind of wavelets we used to build it we have a “perfect” elimination of all geometrical constraints and we find again the pure uncorrelated multiplicative process. On the other hand, had we used a different wavelet basis we would not have obtained in output exactly the same coefficients we put in input. Nevertheless, the physical intuition leads us to the claim that—a part from pathological choices—using wavelets should always clean the spurious effects described by the ward identities (8). An experimental proof supporting this intuition is shown in Fig. 5. In Fig. 5 we show the equivalent of $F_{2,2}(r,R)$ built in terms of the Wavelet coefficients,

$$F_{2,2}^{\text{wav}}(r=2^{-j}, R=2^{-j'}) = \langle |\alpha_{j,k}|^2 |\alpha_{j',k'}|^2 \rangle. \quad (11)$$

In the figure we plot, as in the previous figures, the compensated correlation, obtained from the wavelet coefficients, at fixed small scale and at changing the large scale. In Fig. 6 the same quantities are plotted at changing the small scale. As it is evident, the finite scale-separation effects visible in the standard MSVC have here disappeared; the *plateau* is reached immediately after, say, one fragmentation step.

B. A case where fusion rules fail

For multiscale correlations where the direct application of the random-cascade prediction is useless (because of the

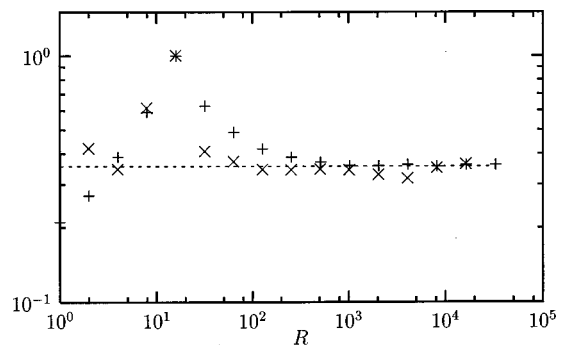


FIG. 5. Comparison between real space (+) and wavelet analysis (x) of the experimental data set from Modane. Compensated $\bar{F}_{2,2}$ is shown for fixed r at varying R .

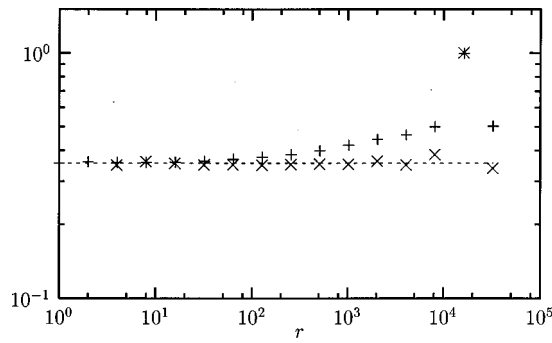


FIG. 6. Comparison between real space (+) and wavelet analysis (x) of the experimental data set from Modane. Compensated $\bar{F}_{2,2}$ is shown for fixed R at varying r .

translation symmetry), like $F_{1,q}(r,R)$, we suppose that the main leading contribution is simply due to the geometrical constraints. In other words, we say that as soon as the main leading effect induced by the presence of a multiplicative random energy transfer is depleted because of symmetry reasons, the subleading contributions induced by the geometry becomes the leading contributions.

In order to give a prediction for such class of MSVC we therefore use the WI applying the multiplicative prediction to all terms, except the $F_{1,q}$. One obtains the expansion

$$F_{1,q}(r,R) \sim \left[O\left(\frac{r}{R}\right)^{\zeta(2)} + O\left(\frac{r}{R}\right)^{\zeta(3)} + O\left(\frac{r}{R}\right)^{\zeta(4)} + \dots + O\left(\frac{r}{R}\right)^{\zeta(q+1)} \right] \cdot S_{q+1}(R), \quad (12)$$

which coincides when $q=1$ with the exact result (9) using $\zeta(3)=1$.

In Fig. 7 we show the experimentally measured $F_{1,2}$ and the fit that we obtain by keeping only the first two terms of the compensated expansion in (12), i.e., $F_{1,2}(r,R)/S_3(R) = (a(r/R)^{\zeta(2)} + b(r/R)^{\zeta(3)})$. The fit has been performed by imposing the value for the scaling exponents $\zeta(2), \zeta(3)$ measured on the structure functions, i.e., only the coefficients in front of the power laws, a, b have been fitted. As one can

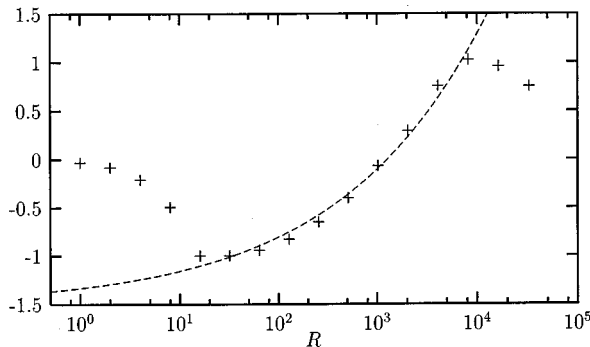


FIG. 7. Experimental $F_{1,2}(r,R)$ at fixed $r=16r_d$ and at varying R . The integral scale $L \sim 1 \times 10^4 r_d$. Let us remark that the observed change of sign in the correlation implies the presence of at least two power laws. The continuous line is the fit in the region $r < R < L$ obtained by using only the first two terms in (12).

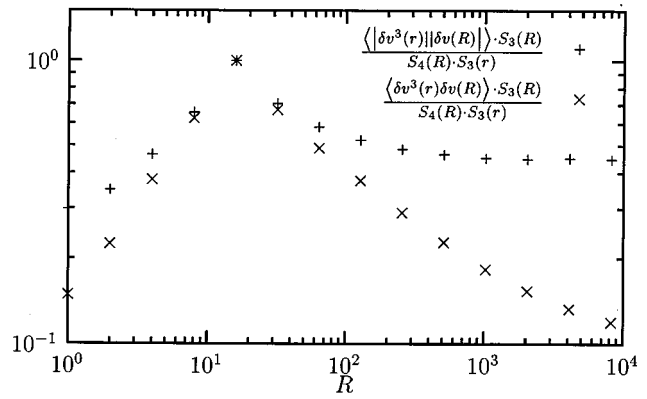


FIG. 8. Comparison between compensated $\bar{F}_{3,1}$ odd MSVC with absolute values (+) and without (x). Data are shown for fixed r at varying R . It is evident that the odd MSVC with absolute values has the same behavior of even MSVC, while the one without absolute value does not follow the same behavior.

notice, the fit works perfectly in the inertial range. Let us remark that the correlation changes sign in the middle of the inertial range, which is a clear indication that a single power-law fit (neglecting subleading terms) would completely miss the correct behavior.

Next we consider the WI for $p=3$. Due to the fact that $S_3(r) \sim r$ in the inertial range, one can easily show that the WI enforces $F_{12} \sim F_{21}$. Therefore, we can safely state that also correlation functions of the form $F_{p,1}$ feel nontrivial dependency from the large scale R , proving that the prediction given in Ref. 8 using isotropy arguments is wrong.

C. Fusion rules: Odd moments

For the most general MSVC involving odd moments of velocity increments, $F_{p,q}(r,R)$ with $p,q=3,5,7,\dots$, the situation is slightly more confused. The problem stems from the fact that the fusion rules contribution to this correlation feels indeed the skewed part of the process which is order of magnitudes less important than the even part. For example, the multiplicative contribution to the correlation $F_{3,1}(r,R)$ would be $S_3(r)/S_3(R) \cdot S_4(R)$ which is different from zero only due to the fact that the process for the longitudinal velocity correlation is skewed.

The weakness of the signal from the multiplicative contributions makes these class of correlation functions very hard to analyze from the point of view of scaling. Here, the geometrical constraints may well be more important, in a large range of scale separation, than the fusion rules prediction. For example in Fig. 8 we plot the standard MSVC for $p=3, q=1$ and the same correlations but with moduli of velocity increments, such as to get rid, in the second case, of cancellation effects. As it is evident, the two correlation have a very different amplitude as soon as the scale separation becomes important and it is hard to say whether the MSVC without moduli follow the fusion rules prediction for large scale separation or not. On the other hand, the correlation with absolute values does follow the multiplicative prediction reaching a plateau after the usual finite size transient as the ordinary even-MSVC.

A high statistics and high Reynolds number investigation of such a class of correlation may well be of some interest in order to elucidate whether the odd part of velocity increments follows the same physics of the even part or not.

IV. DISSIPATIVE PHYSICS

In this section we discuss the application of fusion rules in the dissipative range. We will be mainly interested in the following two quantities:

$$A_n(R) = \langle \Delta v(x) \cdot \delta v_R(x)^n \rangle, \tag{13}$$

$$B_{p,n}(R) = \langle T(x)^p \cdot \delta v_R(x)^n \rangle, \tag{14}$$

where $\Delta v(x)$ is the Laplacian computed at the point x , $\delta v_R(x) = v(x+R) - v(x)$ and $T(x)$ is the velocity gradient computed at x . In order to simplify the discussion we restrict to the one-dimensional case, namely, the Laplacian and the gradient are computed in one dimension and velocity differences are longitudinal. Moreover we restrict our analysis to the cases of n odd and $n+p$ even. Our findings will anyway be valid in the most general case. The scaling properties of A_n and $B_{p,n}$ have been investigated in Refs. 7, 12, and 16.

We start by considering the scaling properties of A_n . By its definition we have

$$\begin{aligned} A_n(R) &= \lim_{r \rightarrow 0} \left\langle \left(\frac{v(x+r) + v(x-r) - 2v(x)}{r^2} \right) \right. \\ &\quad \left. \cdot (v(x+R) - v(x))^n \right\rangle \\ &= \lim_{r \rightarrow 0} r^{-2} (F_{1,n}(r,R) + F_{1,n}(-r,R)). \end{aligned} \tag{15}$$

In order to understand how Eq. (15) works, we compute the easiest quantities, i.e., A_1 and A_3 . By using Eq. (9), we obtain

$$A_1(R) = \lim_{r \rightarrow 0} \frac{r^{-2}}{2} (2S_2(R) + 2S_2(r) - S_2(R-r) - S_2(R+r)) \tag{16}$$

$$= \lim_{r \rightarrow 0} r^{-2} \left(S_2(r) - \frac{1}{2} r^2 \frac{d^2 S_2(R)}{dR^2} + O(r^3) \right) \tag{17}$$

$$= \langle (\partial_x v)^2 \rangle - \frac{1}{2} \frac{d^2 S_2(R)}{dR^2}. \tag{18}$$

In Eq. (18), we have used the relation

$$\langle (\partial_x v)^2 \rangle = \lim_{r \rightarrow 0} \frac{S_2(r)}{r^2}. \tag{19}$$

The computation of A_3 is similar and we find, using Eq. (8),

$$\begin{aligned} A_3(R) &= \lim_{r \rightarrow 0} r^{-2} \frac{1}{4} (2S_4(R) + 2S_4(r) + 12F_{2,2}(r,R) \\ &\quad - 4F_{3,1}(r,R) - 4F_{3,1}(-r,R) \\ &\quad - S_4(R-r) - S_4(R+r)) \end{aligned}$$

$$\begin{aligned} &= \lim_{r \rightarrow 0} r^{-2} \left(3F_{2,2}(r,R) - \frac{1}{4} r^2 \frac{d^2 S_4(R)}{dR^2} + O(r^3) \right) \\ &= 3B_{2,2}(R) - \frac{1}{4} r^2 \frac{d^2 S_4(R)}{dR^2}. \end{aligned} \tag{20}$$

In Eq. (20) we used the definition of $B_{2,2}$, namely,

$$B_{2,2}(R) = \lim_{r \rightarrow 0} r^{-2} F_{2,2}(r,R). \tag{21}$$

At this point it is quite easy to find the most general expression for A_n , which is

$$A_n(R) = nB_{2,n-1}(R) - \frac{1}{n+1} \frac{d^2 S_{n+1}(R)}{dR^2}. \tag{22}$$

Equation (22) is an exact results which is independent on any physical assumption on the fusion rules. The last term on the r.h.s. of (22) becomes small for R in the inertial range. On the other hand, for small value of R , i.e., for $R \rightarrow 0$, the last term of the r.h.s. of (22) cannot be neglected. In particular, for $R \rightarrow 0$, an explicit computation, either using (22) or (13), gives [after cancellations of leading terms in the r.h.s. of (22)],

$$A_n(R) \approx O(R^{n+1}). \tag{23}$$

In order to complete our computation for A_n , we need an estimate for $B_{2,n}$. There are in principle two ways to compute $B_{p,n}$; the first one using the multiscaling approach,¹⁵ the second one using the GESS theory discussed in Ref. 11;

We first analyze the case of multiscaling. In this case, one can use the approach of multiplicative processes with multiscaling viscous cutoff.¹⁵ Namely, for the correlation $B_{2,n}(R) = \langle (\partial_x v)^2 (\delta_R v(x))^n \rangle$ one obtains

$$B_{2,n}(R) \sim \left\langle (\delta_R v(x))^n \left(\frac{\delta_{r_d} v}{r_d} \right)^2 \right\rangle, \tag{24}$$

where r_d is the dissipative scale. In the multifractal interpretation we assume $\delta_{r_d} v = (r_d/R)^h \cdot \delta_R v$ with probability $P_h(r_d, R) = (r_d/R)^{3-D(h)}$. Following Ref. 15 we have

$$\delta_{r_d} v \cdot r_d \sim \left(\frac{r_d}{R} \right)^h \delta_R v \cdot r_d \sim \nu. \tag{25}$$

Inserting the last expression in the definition of $B_{2,n}(R)$, we finally have

$$\begin{aligned} B_{2,n}(R) &\sim \int d\mu(h) \frac{(\delta_R v)^{n+2}}{R^2} \\ &\quad \cdot \left(\frac{\nu}{R \cdot \delta_R v} \right)^{[2(h-1)+3-D(h)]/(1+h)} \sim \frac{S_{n+3}(R)}{\nu \cdot S_3(R)}, \end{aligned} \tag{26}$$

where we have used the fact that the multifractal process is such that $\nu \langle (\partial_x v)^2 \rangle \rightarrow O(1)$ in the limit $\nu \rightarrow 0$. Expression (26) coincides with the prediction given in Ref. 8. The above computation, are easily generalized for any $\langle (\partial_x v)^p (\delta_R v(x))^q \rangle$. By using (26) and (22) we finally obtain

$$A_n(R) = n C_n \frac{S_{n+2}(R)}{\nu S_3(R)} - \frac{1}{n+1} \frac{d^2 S_{n+1}(R)}{dR^2}. \quad (27)$$

Let us note that, for $R \rightarrow 0$ Eq. (27) predicts that $A_n(R) \sim O(R^{n-1})$ which violates Eq. (23).

We now compute $A_n(R)$ by using the GESS approach discussed in Ref. 11. In this case the computation of $B_{2,n}$ can be easily done by noting that, within the GESS approach, the fluctuations of the dissipation scale are confined in the range where $\delta_R v \sim R$. This implies that, for what concerns the scaling properties of $B_{2,n}(R)$, the effect of a fluctuating dissipation scale can be disregarded. Following Ref. 11, after a long but straightforward computation, we obtain

$$B_{2,n}(R) = D_n \frac{\langle T^2 \rangle S_{n+2}(R)}{S_2(R)}, \quad (28)$$

where T is the velocity gradient and D_n is a constant. Equation (28) can be easily understood by noting that, within the GESS approach, $F_{2,n}(r, R) \sim [S_2(r) \cdot S_{n+2}(R)] / S_2(R)$ for any values of r and R , i.e., also in the limit $r \rightarrow 0$. Using (28) we finally obtain

$$A_n(R) = n D_n \frac{\langle T^2 \rangle S_{n+1}(R)}{S_2(R)} - \frac{1}{n+1} \frac{d^2 S_{n+1}(R)}{dR^2}. \quad (29)$$

For $R \rightarrow 0$, using the estimate $S_n(R) \sim \langle T^n \rangle R^n + O(R^{n+2})$, and the fact that $D_n = 1$ for $R = 0$, we can easily show that Eq. (29) satisfies the constrain (23).

From an experimental point of view, it is extremely difficult to distinguish between the two predictions (27) or (29). We note that the experimental and numerical analysis discussed in Refs. 12 and 13, has been done neglecting the second term on the r.h.s. of (22). Also, the experimental analysis performed in Ref. 11 seems to indicate that multiscale effects are not observed in real turbulence. At any rate, no definitive conclusions can be drawn from existing experimental data. A third, different parameterization of viscous effects has also been presented in Ref. 22.

V. CONCLUSIONS

Let us summarize what is the framework we have found until now.

Whenever the simple scaling *ansatz* based on the uncorrelated multiplicative process is not prevented by symmetry arguments, the multiscale correlations are in good asymptotic agreement with the fusion rules prediction even if strong corrections due to subleading terms are seen for small-scale separation $r/R \sim O(1)$. Subleading terms are strongly connected to the WI previously discussed, i.e., to geometrical constraints. In the other cases [i.e., $F_{1,q}(r, R)$] the geometry fully determines both leading and subleading scaling. All these findings, led us to the conclusions that multiscale correlations functions measured in turbulence are fully consistent with a multiplicative, almost uncorrelated, random process. Nevertheless, the strong and slowly-decaying subleading corrections to the naive multiplicative fusion rules predictions are the main obstacle for any attempts to attack analytically the equation of motion for structure functions; in that case, multiscale correlations at almost

coinciding scales are certainly the dominant contributions in the nonlinear part of the equations.⁸ Indeed, as shown in an analytical calculation for a dynamical toy model of random passive-scalar advection,²⁰ fusion rules are violated at small scale-separation and the violations are relevant for correctly evaluating the exact behavior of structure functions at all scales.

Finally, let us remark that the standard multiplicative process cannot be the end of the story, i.e., the dynamics is certainly more complex than what here summarized. For example, one cannot exclude that also subleading (with respect to the multiplicative *ansatz*) dynamical processes are acting in the energy transfer from large to small scales. These dynamical corrections must be either negligible with respect to the geometrical constraints or, at best, of the same order. As already discussed, a better understanding of this small deviations is necessary in order to improve our analytic control of intermittent deviations in Navier–Stokes equations. Let us cite, for example, a previous attempt, made by some of the authors, to close the equation of motion in a dynamical model of turbulence by using a simple multiplicative process.²⁸ In that case, one was able to find a satisfactory qualitative agreement with the numerical simulations and at the same time one could also prove that the closure was not exact due to the presence of small out of control, deviations from the multiplicative *ansatz*. Unfortunately, these deviations, as shown in this paper, are hardly detectable experimentally. Also, as shown in Sec. III C, the odd correlation functions are not fully understood; higher Reynolds number experiments, with higher statistics, are needed.

The question connected to the transfer properties of quantities with different physical dimension from the energy, say the helicity, may reveal different physical mechanisms.²⁵ What happens for all those multiscale correlation functions which feel a nontrivial helicity dependency for nonparity invariant flows is in this framework an open question.

In the past, similar analysis in a class of multiplicative models for the energy dissipation have been done.²⁶ Also in that case, the multipliers connecting coarse-grained energy dissipation over two overlapping intervals shows some weak correlations among scales. This correlation can also be understood in terms of unavoidable geometrical effects due to the overlapping nature of the intervals where the coarse-grained energy dissipation is defined.

For what concerns fusion rules involving velocity gradients or Laplacian and velocity differences, we observe that there are controversial arguments leading to different predictions. It is difficult to distinguish which predictions is really observed in real turbulence, because experimental data at large Reynolds number do not resolve the far dissipative range with enough accuracy.

Finally, let us mention that other possible candidates to investigate the previous problems are shell models for turbulence, where geometrical constraints do not affect the energy cascade mechanism.

ACKNOWLEDGMENTS

We acknowledge useful discussions with A. L. Fairhall, V. L'vov, and I. Procaccia. M. Pasqui is kindly acknowl-

edged for his help in the analysis of the synthetic signal. We are indebted to Y. Gagne for having allowed us the access to the experimental data. L.B. and F.T. have been supported by INFM (PRA TURBO). G.R.C. and S.C. acknowledge support by ECOS comitee and CONACYT under Project No. M96-E03.

APPENDIX: SYNTHETIC SIGNALS

We build up a one-dimensional synthetic signal according to a random multiplicative process defined in a dyadic hierarchical structure as originally introduced in Ref. 14 (for a review and references see also Ref. 21).

Let us consider a wavelet decomposition of the function $\phi(x)$,

$$\phi(x) = \sum_{j,k=0}^{\infty} \alpha_{j,k} \psi_{j,k}(x), \tag{A1}$$

where $\psi_{j,k}(x) = 2^{j/2} \psi(2^j x - k)$ and $\psi(x)$ is any wavelet with zero mean. The above decomposition defines the signal as a dyadic superposition of basic fluctuations with different characteristic widths (controlled by the index j) and centered in different spatial points (controlled by the index k). For functions defined on $N = 2^n$ points in the interval $[0, 1]$ the sums in (A1) are restricted from zero to $n - 1$ for the index j and from zero to $2^j - 1$ for k .

In Ref. 14 it has been shown that the statistical behavior of signal increments,

$$\langle |\delta\phi(r)|^p \rangle = \langle |\phi(x+r) - \phi(x)|^p \rangle \sim r^{\zeta(p)}$$

is controlled by the coefficients $\alpha_{j,k}$. By defining the α coefficients in terms of a multiplicative random process on the dyadic tree it is possible to give an explicit expression for the scaling exponents $\zeta(p)$. For example, it is possible to recover the standard anomalous scaling by defining the α 's tree in term of the realizations of a random variable η with a probability distribution $P(\eta)$,

$$\begin{aligned} \alpha_{0,0} &= \text{const.} \\ \alpha_{1,0} &= \eta_{1,0} \alpha_{0,0}; & \alpha_{1,1} &= \eta_{1,1} \alpha_{0,0}; \\ \alpha_{2,0} &= \eta_{2,0} \alpha_{1,0}; & \alpha_{2,1} &= \eta_{2,1} \alpha_{1,0}; \\ \alpha_{2,2} &= \eta_{2,2} \alpha_{1,1}; & \alpha_{2,3} &= \eta_{2,3} \alpha_{1,1}; \end{aligned} \tag{A2}$$

and so on. Let us note that in the previous multiplicative process different scales are characterized by different values of the index j , i.e., $r_j = 2^{-j}$. If the $\eta_{j,k}$ are independent identically distributed random variables it is straightforward to realize that $\alpha_{j,k}$ are random variables with moments given by

$$\langle |\alpha_{j,k}|^p \rangle = r_j^{-\log_2(\overline{\eta^p})} = r_j^{\zeta(p)}, \tag{A3}$$

where the ‘‘mother eddy’’ $\alpha_{0,0}$ has been chosen to be equal to one. In (A3) with \dots we intend averaging over the $P(\eta)$ distribution. In Ref. 14 it has been shown that also the signal $\phi(x)$ has the same anomalous scaling of (A3).

The same arguments used in order to prove that the field $\phi(x)$ has an anomalous scaling can be invoked to show also that the fusion-rules prediction (5) are satisfied -at least for large scale separation-

On the other hand, it is trivial matter to realize that the above signal will show *exactly*, and *for any* separation of scale, the fusion-rules prediction if expressed for the wavelet coefficients $\alpha_{j,k}$. For example, let us consider two wavelet coefficients at different scales $r_j < r_{j'}$, and let us chose the k indices such that the two coefficients refer to two spatially overlapping wavelets, then it is trivial to realize that, due to the multiplicative nature of the wavelet coefficients, we have

$$\langle |\alpha_{j,k}|^p |\alpha_{j',k'}|^q \rangle \equiv \left(\frac{r_j}{r_{j'}} \right)^{\xi(p)} r_{j'}^{\xi(p+q)} \tag{A4}$$

which shows that the fusion rules prediction is satisfied exactly for any separation of scales as long as the two fluctuations are chosen with overlapping distances. In the case the two distances are not overlapping, deviations from the fusion rules prediction are certainly seen in the synthetic field due to the dyadic (ultrametric) nature of the underlying structure. The question whether such deviations may be seen also in the experimental data is an interesting point which is outside the scope of this paper (see, for similar problems, Refs. 23, 24).

Other synthetic signals²⁷ can be built either starting by a multiplicative process from the energy dissipation, and using the refined Kolmogorov hypothesis in order to have a signal for the velocity, or by using ‘‘wavelet-like’’ tent functions. Our signal, focusing directly on the velocity fields increments, without passing from the energy dissipation, and being infinitely differentiable, at difference from the tent-function signal, looks more appropriate for our purposes.

¹U. Frisch, *Turbulence: The Legacy of A. N. Kolmogorov* (Cambridge University Press, Cambridge, 1995).
²R. H. Kraichnan, ‘‘Lagrangian-history closure approximation for turbulence,’’ *Phys. Fluids* **8**, 575 (1965).
³V. I. Belinicher and V. L’vov, ‘‘A scale invariant theory of fully developed hydrodynamic turbulence,’’ *Sov. Phys. JETP* **66**, 303 (1987).
⁴C. Meneveau and T. S. Lund, ‘‘On the Lagrangian nature of the energy cascade,’’ *Phys. Fluids* **6**, 8 (1994).
⁵L. Biferale, G. Boffetta, A. Celani, and F. Toschi, ‘‘Multitime multiscale correlation functions in turbulence and in turbulent models,’’ *Physica D* **127**, 187 (1999).
⁶G. Eyink, ‘‘Lagrangian field theory, multifractals, and universal scaling in turbulence,’’ *Phys. Lett. A* **172**, 355 (1993).
⁷V. S. L’vov and I. Procaccia, ‘‘Fusion rules in turbulent systems with flux equilibrium,’’ *Phys. Rev. Lett.* **76**, 2898 (1996).
⁸V. S. L’vov and I. Procaccia, ‘‘Toward a nonperturbative theory of hydrodynamic turbulence: Fusion rules, exact bridge relations, and anomalous viscous scaling functions,’’ *Phys. Rev. E* **54**, 6268 (1996).
⁹V. L’vov, E. Podivilov, and I. Procaccia, ‘‘Temporal multiscaling in hydrodynamic turbulence,’’ *Phys. Rev. E* **55**, 7030 (1997).
¹⁰A. L. Fairhall, B. Druva, V. S. L’vov, I. Procaccia, and K. S. Sreenivasan, ‘‘Fusion rules in Navier–Stokes turbulence: First experimental tests,’’ *Phys. Rev. Lett.* **79**, 3174 (1997).
¹¹R. Benzi, L. Biferale, S. Ciliberto, M. V. Struglia, and R. Tripiccone, ‘‘A generalized scaling of fully developed turbulence,’’ *Physica D* **96**, 162 (1996).
¹²A. L. Fairhall, V. S. L’vov, and I. Procaccia, ‘‘Dissipative scaling functions in Navier–Stokes turbulence: Experimental tests,’’ *chao-dyn/9709034* (unpublished).
¹³A. Celani and D. Biskamp, ‘‘Bridge relations in Navier–Stokes turbulence,’’ *chao-dyn/9806027* (unpublished).
¹⁴R. Benzi, L. Biferale, A. Crisanti, G. Paladin, M. Vergassola, and A. Vulpiani, ‘‘A random process for the construction of a multiaffine field,’’ *Physica D* **65**, 352 (1993).
¹⁵U. Frisch and M. Vergassola, ‘‘A prediction of the multifractal model: The intermediate dissipation range,’’ *Europhys. Lett.* **14**, 439 (1991).

- ¹⁶R. Benzi, L. Biferale, and F. Toschi, "Multiscale correlation functions in turbulence," *Phys. Rev. Lett.* **80**, 3244 (1998).
- ¹⁷H. Kahaleras, Y. Malecot, Y. Gagne, and B. Castaing, "Intermittency and Reynolds number," *Phys. Fluids* **10**, 910 (1998).
- ¹⁸R. Benzi, S. Ciliberto, C. Baudet, and G. Ruiz-Chavarria, "On the scaling of three-dimensional homogeneous and isotropic turbulence," *Physica D* **80**, 385 (1994).
- ¹⁹R. Benzi, F. Toschi, and R. Tripiccone, "On the heat transfer in Rayleigh-Bénard systems," *J. Stat. Phys.* **93**, 901 (1998).
- ²⁰R. Benzi, L. Biferale, and A. Wirth, "Analytic calculation of anomalous scaling in random shell models for a passive scalar," *Phys. Rev. Lett.* **78**, 4926 (1997).
- ²¹G. Stolovitzky and K. R. Sreenivasan, "Kolmogorov's refined similarity hypothesis for turbulence and general stochastic processes," *Rev. Mod. Phys.* **66**, 229 (1994).
- ²²G. Stolovitzky, K. R. Sreenivasan, and A. Juneja, "Scaling functions and scaling exponents in turbulence," *Phys. Rev. E* **48**, R3217 (1993).
- ²³R. Benzi, L. Biferale, and E. Trovatore, "Ultrametric structure of multi-scale energy correlations in turbulent models," *Phys. Rev. Lett.* **79**, 1670 (1997).
- ²⁴J. O'Neil and C. Meneveau, "Spatial correlations in turbulence: Predictions from multifractal formalism and comparison with experiments," *Phys. Fluids A* **5**, 158 (1993).
- ²⁵L. Biferale, D. Pierotti, and F. Toschi, "Helicity transfer in dynamical models for turbulence," *Phys. Rev. E* **57**, R2515 (1998).
- ²⁶K. R. Sreenivasan and G. Stolovitzky, "Turbulent cascades," *J. Stat. Phys.* **78**, 311 (1995).
- ²⁷A. Juneja, D. P. Lathrop, K. R. Sreenivasan, and G. Stolovitzky, "Synthetic turbulence," *Phys. Rev. E* **49**, 5179 (1994).
- ²⁸R. Benzi, L. Biferale, and G. Parisi, "On intermittency in a cascade model for turbulence," *Physica D* **65**, 163 (1993).